

# Theoretical study of P-wave molecular states

报告人：王俊璋（重庆大学）



**基于工作：** Phys. Rev. Lett. 133, 241903 (2024) and Phys. Rev. D 110 (2024) 11, 114003.

**合作者包括：** 林子阳，程剑波，王波，孟璐博士和朱世琳教授

2025.07.04 湖南科技大学@湘潭

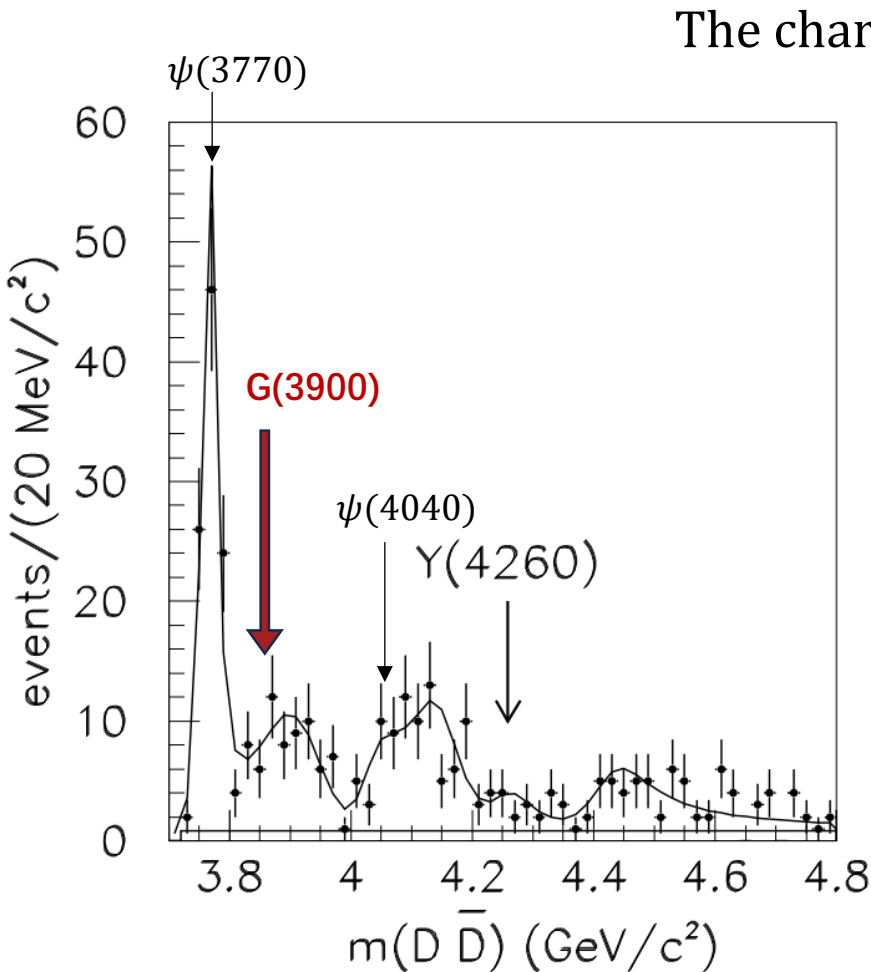
# Outline

---

- P-wave  $D\bar{D}^*$  resonance candidate:  $G(3900)$
- P-wave resonance mechanism
- Robustness for the existence of P-wave vector  $D\bar{D}^*$  resonance
- $X_1(2900)$  as the P-wave  $\bar{D}^*K^*$  resonance
- Outlook: studying general behavior of P-wave hadron-hadron scattering at STCF

# Motivation--Cross Sections for $e^+e^- \rightarrow D\bar{D}$

- Broad structure near  $D\bar{D}^*$  threshold, referred to as **G(3900) structure**



(BaBar Collaboration), Phys. Rev. D 76, 111105 (2007),

The charmoniumlike state with  $J^{PC} = 1^{--}$

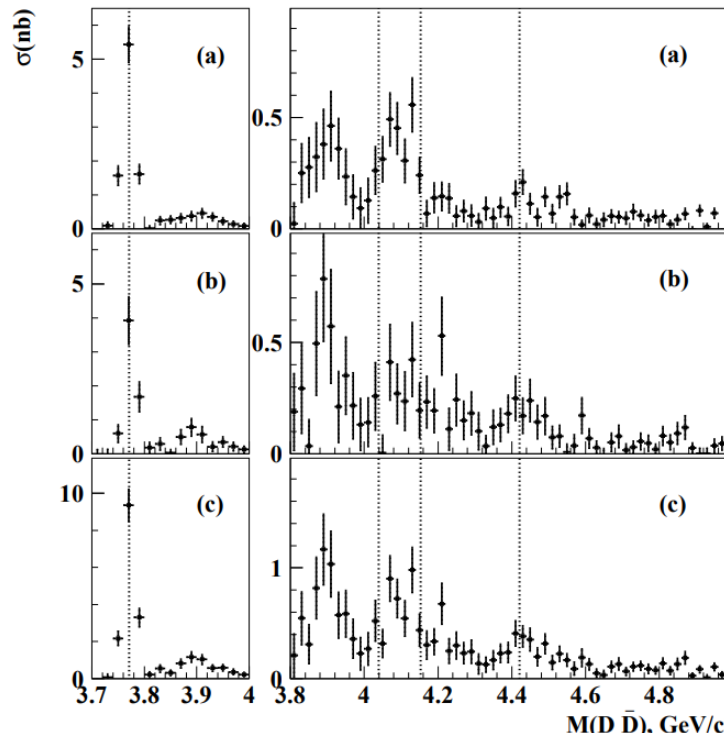
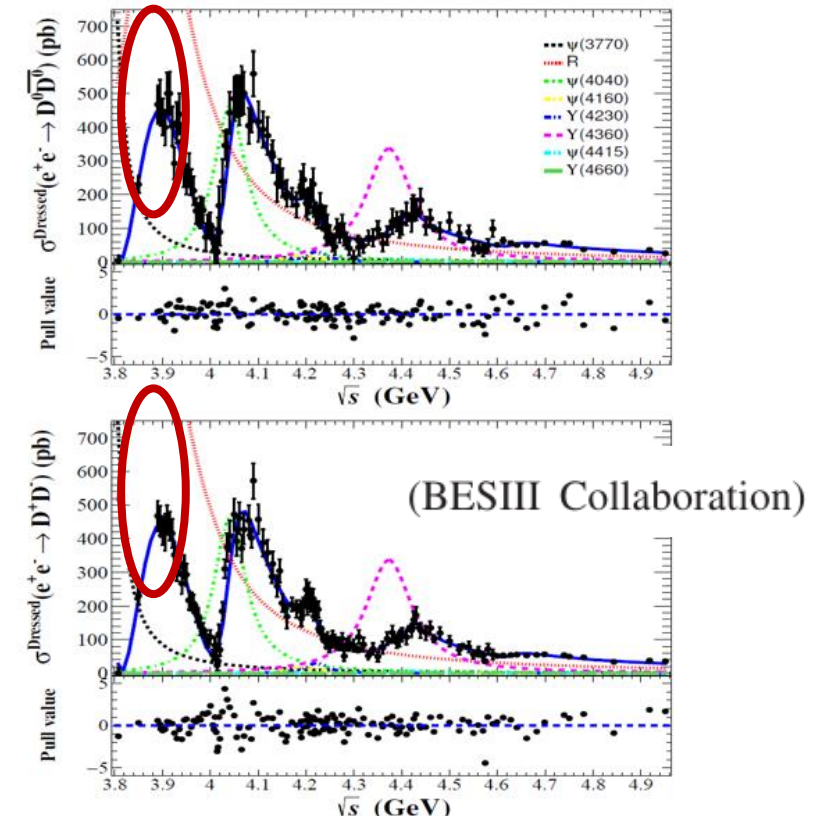


FIG. 3: The exclusive cross sections for: (a)  $e^+e^- \rightarrow D^0\bar{D}^0$ ; (b)  $e^+e^- \rightarrow D^+\bar{D}^-$ ; (c)  $e^+e^- \rightarrow D\bar{D}$ . The dotted lines correspond to the  $\psi(3770)$ ,  $\psi(4040)$ ,  $\psi(4160)$  and  $\psi(4415)$  masses [20].

(Belle Collaboration), Phys. Rev. D 77, 011103 (2008)

fitted with Gaussian function



Mass:  $3872.5 \pm 14.2 \pm 3.0$  MeV

Width:  $179.7 \pm 14.1 \pm 7.0$  MeV  
 $S(\sigma) > 20$



# Background-G(3900)

PHYSICAL REVIEW D

VOLUME 21, NUMBER 1

1 JANUARY 1980

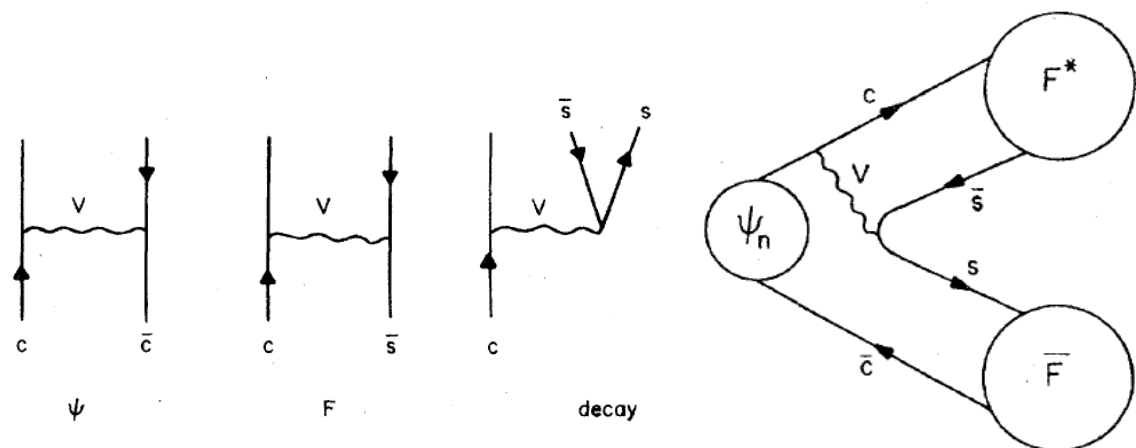
## Charmonium: Comparison with experiment

E. Eichten,\* K. Gottfried, T. Kinoshita, K. D. Lane,\* and T. M. Yan

Laboratory of Nuclear Studies, Cornell University, Ithaca, New York 14853

(Received 25 June 1979)

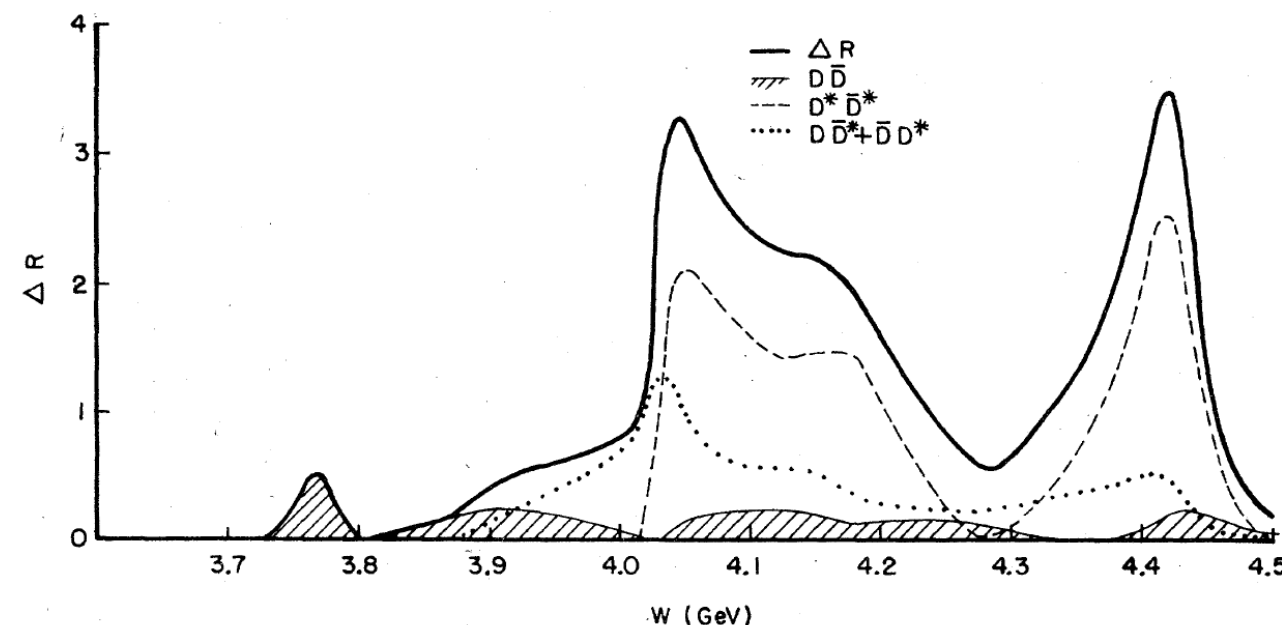
The charmonium model, formulated in detail in an earlier publication, is compared in a comprehensive fashion with the data on the  $\psi$  family. The parameters of the "naive" model, in which the system is described as a  $c\bar{c}$  pair, are determined from the observed positions of  $\psi$ ,  $\psi'$ , and the  $P$  states. The model then yields a successful description of the spectrum of spin-triplet states above the charm threshold. It also accounts for the ratio of the leptonic widths of  $\psi'$  and  $\psi$ . When the  $c\bar{c}$  potential is applied to the  $T$  family, it accounts, without any readjustment of parameters, for the positions of the  $2S$  and  $3S$  levels and for the leptonic widths of  $T$  and  $T'$  relative to that of  $\psi$ . The model does not give acceptable values of the absolute leptonic widths, a shortcoming which is ascribed to large quantum-chromodynamic corrections to the van Royen-Weisskopf formula. The calculated  $E1$  rates are about twice the values observed in the  $\psi$  family. This naive model is also extended with considerable success to mesons composed of one heavy and one light quark. A significant extension of the model is achieved by incorporating coupling to charmed-meson decay channels. This gives a satisfactory understanding of  $\psi(3772)$  as the  $1^3D_1$   $c\bar{c}$  state, mixed via open and closed decay channels to  $2^3S$ . The model has decay amplitudes that are oscillatory functions of the decay momentum; these oscillations are a direct consequence of the radial nodes in the  $c\bar{c}$  parent states. These amplitudes provide a qualitative understanding of the observed peculiar branching ratios into various charmed-meson channels near the resonance at 4.03 GeV, which is assigned to  $3^3S$ . The coupling of the  $c\bar{c}$  states below the charm threshold to closed decay channels modifies the bound states and leads to reduction of about 20% in  $E1$  rates in comparison to those of th



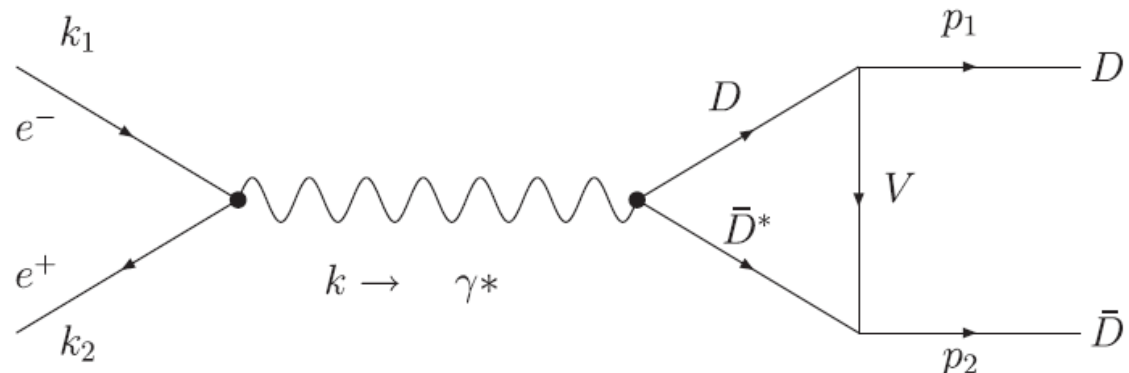
## Cornell model

$$V(r) = -\frac{\kappa}{r} + \frac{r}{a^2},$$

$$H_t = \frac{3}{8} \sum_{a=1}^8 \int : \rho_a(\vec{r}) V(\vec{r} - \vec{r}') \rho_a(\vec{r}') : d^3 r d^3 r', \quad (3.1)$$



- kinematic effect at the threshold

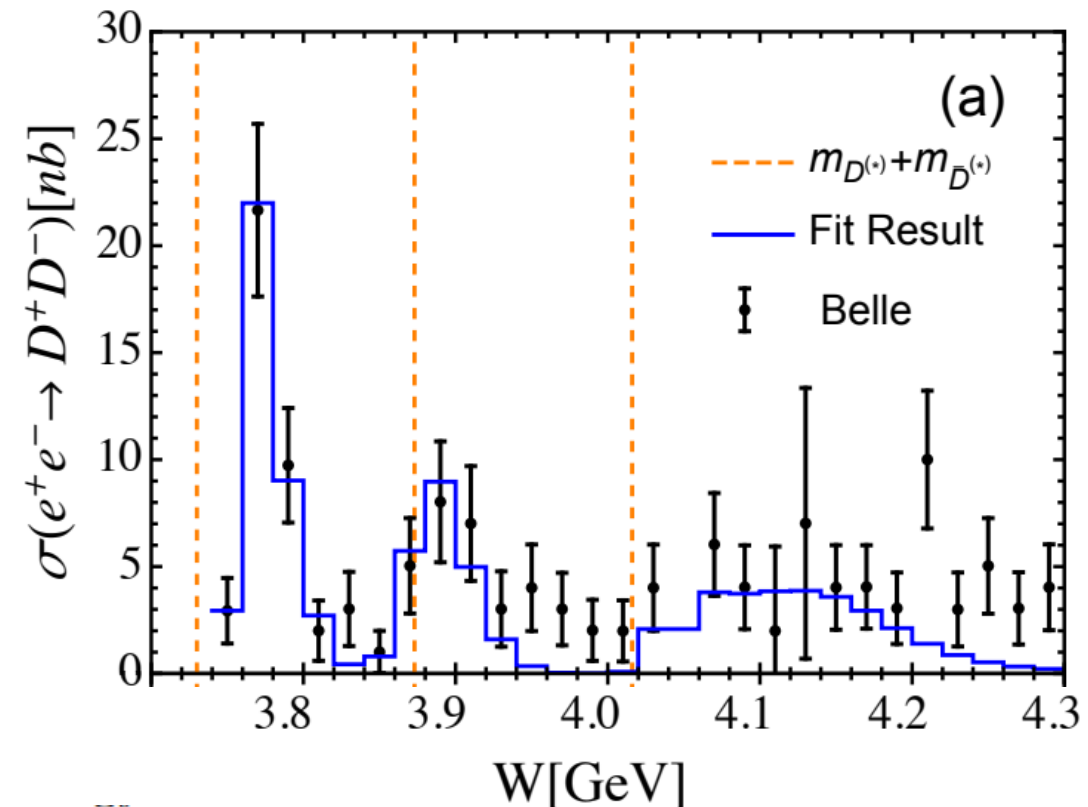


Y.J. Zhang and Q. Zhao,  
Phys. Rev. D 81, 034011 (2010)

- coupled-channel effects driven by the contact interactions

$$\psi(2S), \psi(3S), \psi(1D), \psi(2D) \otimes D\bar{D}, D\bar{D}^* + c.c., D^*\bar{D}_{s=0}^*$$

M.L. Du, U. G. Meissner and Q. Wang Phys. Rev.  
D 94 (2016) 9, 096006

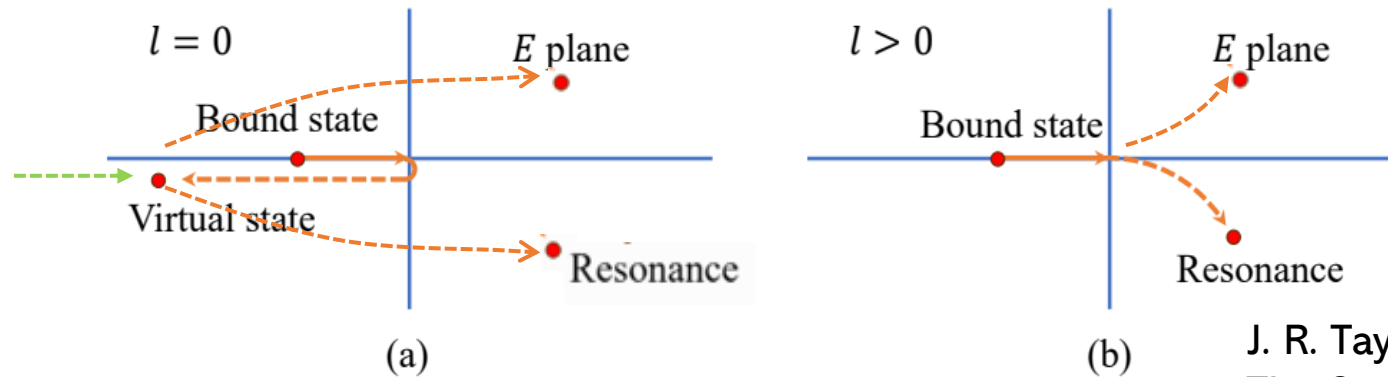


Sheet	Poles (GeV)	$ g_{D\bar{D}} $	$ g_{D\bar{D}^*} $	$ g_{D^*\bar{D}_{s=0}^*} $	$ g_{D^*\bar{D}_{s=2}^*} $
II	$3.764 \pm i0.006$	13.53	9.48	5.88	16.78
III	$3.879 \pm i0.035$	4.40	10.96	7.63	18.15
IV	$4.034 \pm i0.014$	2.90	2.23	12.52	12.85

# Formalism – P-wave resonance



## P-wave resonance mechanism



J. R. Taylor, Scattering Theory:  
The Quantum Theory of Nonrelativistic Collision

- As the attraction being weaker, p-wave bound state naturally turns resonances.
- This resonance is different to Feshbach resonance (bound states coupled with open channels)

# The dynamical calculation of the P-wave $D\bar{D}^*$ interaction

## A basic idea:

- By applying a model, the  $D\bar{D}^*$  interaction can be restricted by the well-known S-wave  $X(3872)$  or  $T_{cc}$ .
- Thus, the prediction on the corresponding P-wave dimeson states should be reliable.
- The predictions on possible P-wave  $D\bar{D}^*$  poles are fully based on a dynamical calculation, which does not depend any experimental information of  $G(3900)$ .

# Formalism – OBE model

- The hadron-hadron interactions are fulfilled with pseudoscalar and vector meson exchange
- The OBE model had succeed in describing the  $X(3872)$  and predicting the existence of  $T_{cc}^+$ .**
- Our work proves that the  $Z_c(3900)$  can also be interpreted as virtual state in OBE model.

$$\begin{aligned}\mathcal{L} = & g_s \text{Tr} [\mathcal{H} \sigma \bar{\mathcal{H}}] + ig_a \text{Tr} [\mathcal{H} \gamma_\mu \gamma_5 \mathcal{A}^\mu \bar{\mathcal{H}}] \\ & + i\beta \text{Tr} [\mathcal{H} v_\mu (\mathcal{V}^\mu - \rho^\mu) \bar{\mathcal{H}}] + i\lambda \text{Tr} [\mathcal{H} \sigma_{\mu\nu} F^{\mu\nu} \bar{\mathcal{H}}] \\ & + g_s \text{Tr} [\bar{\tilde{\mathcal{H}}} \sigma \tilde{\mathcal{H}}] + ig_a \text{Tr} [\bar{\tilde{\mathcal{H}}} \gamma_\mu \gamma_5 \mathcal{A}^\mu \tilde{\mathcal{H}}] \\ & - i\beta \text{Tr} [\bar{\tilde{\mathcal{H}}} v_\mu (\mathcal{V}^\mu - \rho^\mu) \tilde{\mathcal{H}}] + i\lambda \text{Tr} [\bar{\tilde{\mathcal{H}}} \sigma_{\mu\nu} F^{\mu\nu} \tilde{\mathcal{H}}]\end{aligned}$$

OBE model  
( $\pi, \eta, \sigma, \rho, \omega$ )

$$\rho^\mu = \frac{ig_V}{\sqrt{2}} \begin{pmatrix} \frac{\rho_0}{\sqrt{2}} + \frac{\omega}{\sqrt{2}} & \rho^+ \\ \rho^- & -\frac{\rho_0}{\sqrt{2}} + \frac{\omega}{\sqrt{2}} \end{pmatrix}^\mu, \quad \mathbb{P} = \begin{pmatrix} \frac{\pi_0}{\sqrt{2}} + \frac{\eta}{\sqrt{6}} & \pi^+ \\ \pi^- & -\frac{\pi_0}{\sqrt{2}} + \frac{\eta}{\sqrt{6}} \end{pmatrix}.$$

$$\begin{aligned}\mathcal{V}^\mu &= \frac{1}{2}[\xi^\dagger, \partial_\mu \xi], \quad \mathcal{A}^\mu = \frac{1}{2}\{\xi^\dagger, \partial_\mu \xi\} \\ \xi &= \exp(i\mathbb{P}/f_\pi).\end{aligned} \quad F^{\mu\nu} = \partial^\mu \rho^\nu - \partial^\nu \rho^\mu - [\rho^\mu, \rho^\nu]$$

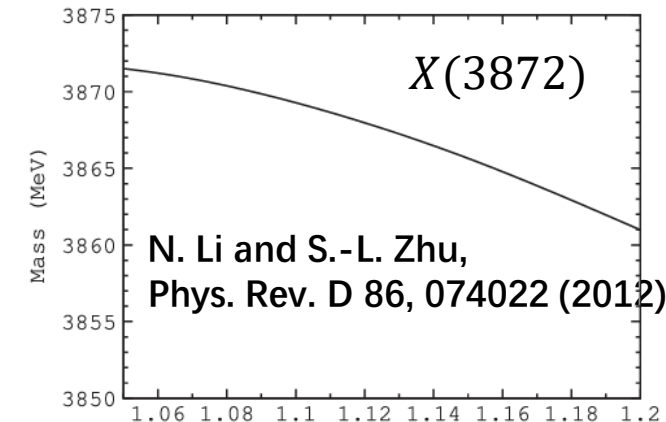


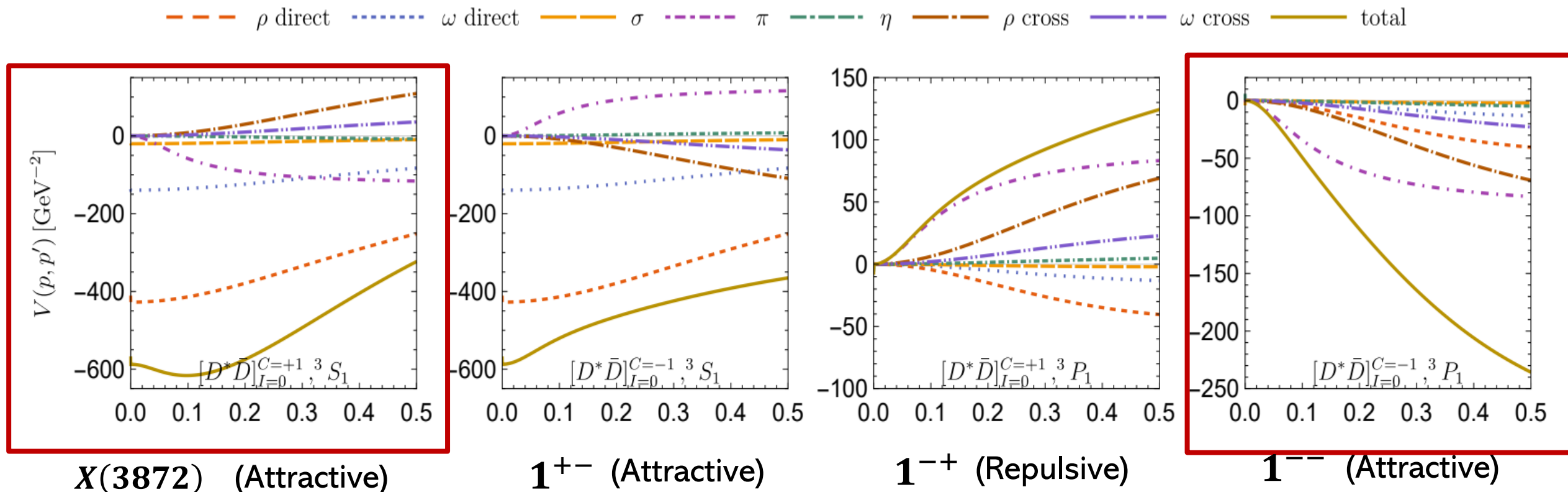
TABLE IV. The numerical results for the  $D^{(*)}D^{(*)}$  system. “\* \* \*” means the corresponding state does not exist due to symmetry while “. . .” means there does not exist binding energy with the cutoff parameter less than 3.0 GeV. The binding energies for the states  $D^{(*)}D^{(*)}[I(J^P) = 0(1^+)]$  and  $D^{(*)}D^{(*)}[I(J^P) = 1(1^+)]$  are relative to the threshold of  $DD^*$  while that of the state  $D^{(*)}D^{(*)}[I(J^P) = 1(0^+)]$  is relative to the  $DD$  threshold.

$I$	$J^P$	$T_{cc}^+$		$D^{(*)}D^{(*)}$						OBE	
				OPE				$D^{(*)}D^{(*)}$			
		$\Lambda$ (GeV)	B.E. (MeV)	1.05	1.10	1.15	1.20	0.95	1.00	1.05	1.10
0	1 <sup>+</sup>	M (MeV)	3874.61	3871.22	3864.83	3854.87	3875.38	3870.41	3857.13	3833.03	42.82
		$r_{\text{rms}}$ (fm)	3.11	1.68	1.12	0.84	4.46	1.58	0.91	0.64	
		$P_1$ (%)	96.39	92.71	88.22	83.34	97.97	92.94	85.64	77.88	
		$P_2$ (%)	0.73	0.72	0.57	0.42	0.58	0.55	0.32	0.15	
		$P_3$ (%)	2.79	6.45	11.07	16.11	1.41	6.42	13.97	21.91	
		$P_4$ (%)	0.08	0.13	0.14	0.13	0.04	0.09	0.08	0.05	

N. Li, Z.-F. Sun, X. Liu, and S.-L. Zhu Phys. Rev. D 88, 114008 (2013)

# The partial-wave $D\bar{D}^*$ interaction( $l=0$ )

Partial-wave potentials  $V(p, p')$  for different exchanged mesons: ( $p' = p$  in the figure)



The P-wave interaction is dominated by the long-distance pion-exchange.

# Unified description of $D\bar{D}^*/DD^*$ molecules

- Poles derived by complex scaling method / Lippmann-Schwinger equation
- Fix the cutoff to simultaneously generate loosely bound  $X(3872)$ ,  $T_{cc}^+$ , we obtain:
  1. **virtual state**  $Z_c(3900)$
  2. a new pole: **p-wave resonance  $G(3900)$**
- Potentials can be related each other
- The same set of parameters

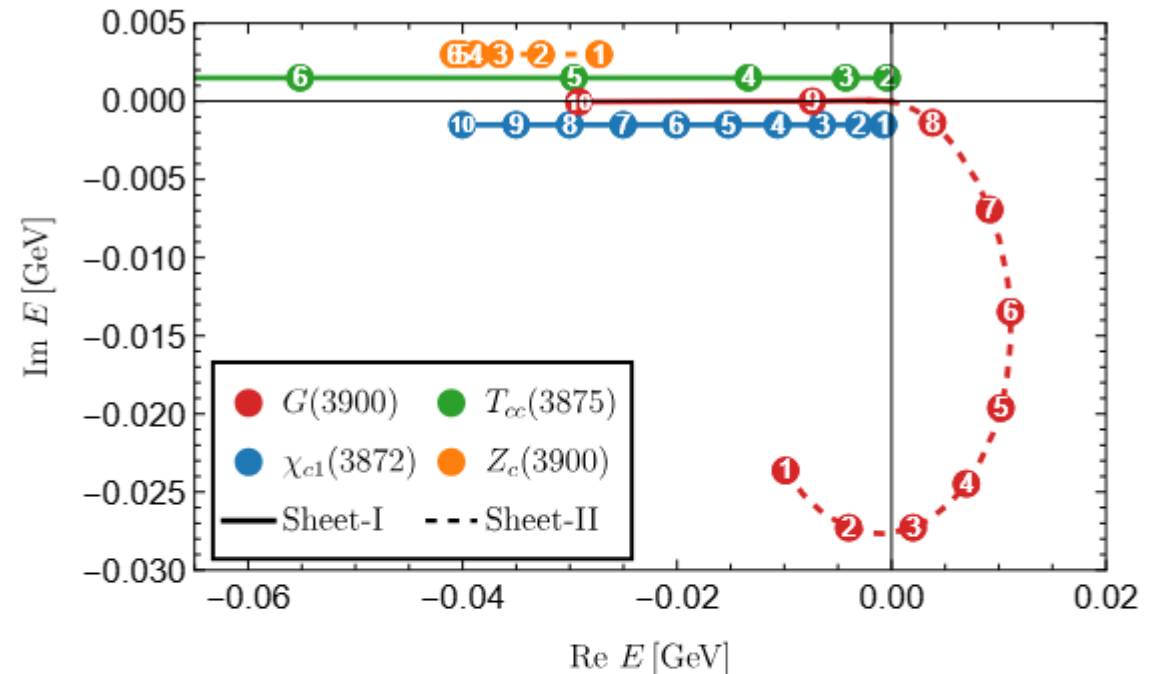


FIG. 4. The pole trajectories with the cutoff parameters correspond to  $\chi_{c1}(3872)$ ,  $T_{cc}(3875)$ ,  $Z_c(3900)$  and the newly observed  $G(3900)$  states. The circled number 1-10 represent the increasing cutoff 0.4-1.3 GeV in order. The solid (dashed) lines represent the pole trajectories in the physical (unphysical) Riemann sheets. The poles on the negative real axis are slightly shifted for transparency.

# More P-wave $D\bar{D}^*$ molecular resonances

TABLE I. The poles in all channels of  $D\bar{D}^*$  and  $DD^*$ , up to the orbital angular momentum  $L = 1$ . The  $B$  and  $V$  superscripts denote the bound state and the virtual state, respectively. Otherwise the pole refers to a resonance.

		$D\bar{D}^*, C = +$		$D\bar{D}^*, C = -$		$DD^*$	
		$I = 0$	$I = 1$	$I = 0$	$I = 1$	$I = 0$	$I = 1$
$\Lambda = 0.5\text{GeV}$	$1^+({}^3S_1)$	$-3.1^B, \chi_{c1}(3872)$	-	$-1.60^B$	$-35.6^V, Z_c(3900)$	$-0.41^B, T_{cc}(3875)$	-
	$0^-({}^3P_0)$	$-1.5 - 14.5i$	-	-	-	$-9.6 - 9.7i$	-
	$1^-({}^3P_1)$	-	-	$-4.0 - 27.3i, Y(3872)$	-	$-31.7 - 70.6i$	-
$\Lambda = 0.6\text{GeV}$	$2^-({}^3P_2)$	$-42.6 - 39.4i$	-	$-21.3 - 50.7i$	-	$-37.8 - 40.9i$	-
	$1^+({}^3S_1)$	$-6.5^B, \chi_{c1}(3872)$	-	$-5.8^B$	$-34.6^V, Z_c(3900)$	$-4.3^B, T_{cc}(3875)$	-
	$0^-({}^3P_0)$	$3.2 - 13.7i$	-	-	-	$-10.2 - 12.1i$	-
	$1^-({}^3P_1)$	-	-	$2.0 - 27.3i, Y(3872)$	-	$-33.7 - 84.8i$	-
	$2^-({}^3P_2)$	$-44.2 - 49.0i$	-	$-19.3 - 58.8i$	-	$-37.8 - 49.3i$	-

**1<sup>+-</sup>:**  $\eta_c\omega, J/\psi\eta, J/\psi\pi\pi$

**0<sup>-+</sup>:**  $\eta_c\pi\pi, J/\psi\omega, \chi_{c1}\pi\pi$

**2<sup>-+</sup>:**  $J/\psi\omega, \chi_{c1}\pi\pi$

**2<sup>--</sup>:**  $\eta_c\omega, J/\psi\eta$

# Discussion – Robustness of our conclusion

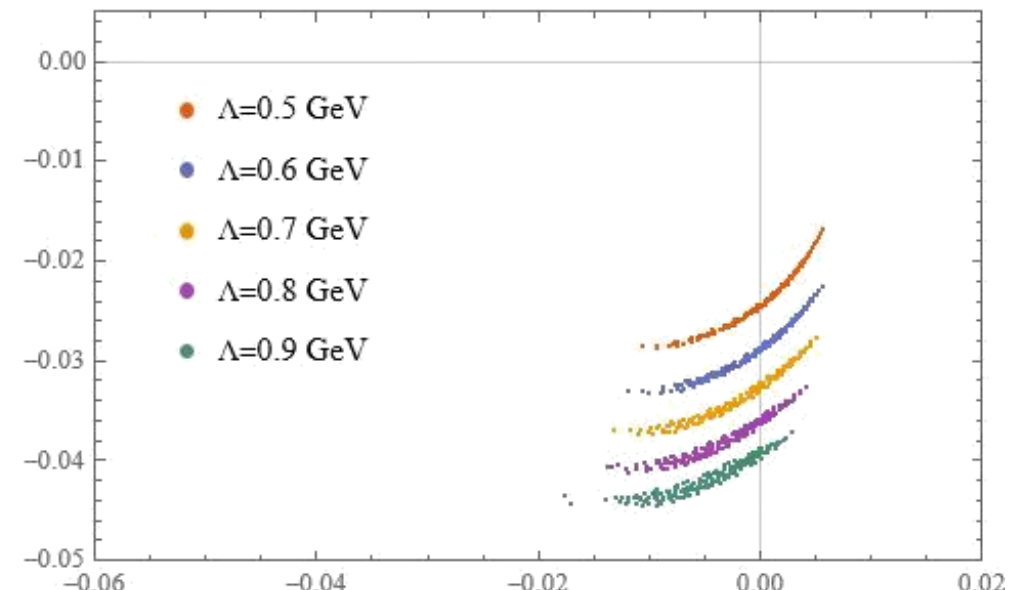
- Higher partial waves are dominant by **long-range** interactions (one pion exchange)
- P-wave interactions fixed by S-wave states ----- **cutoff independent**
- We study the theoretical systematic uncertainty from coupling constants in model.
- We also test the influence of coupled-channel effects, three-body effects and recoil correction (spin-orbit force) on  $G(3900)$ .

# Robustness of our conclusion-coupling constant

- Randomly adjust the coupling constants in OBE to reproduce a shallow bound  $T_{cc}$  and  $X(3872)$

$$\begin{aligned}\mathcal{L} = & g_s \text{Tr} [\mathcal{H} \sigma \bar{\mathcal{H}}] + i g_a \text{Tr} [\mathcal{H} \gamma_\mu \gamma_5 A^\mu \bar{\mathcal{H}}] \\ & + i\beta \text{Tr} [\mathcal{H} v_\mu (\mathcal{V}^\mu - \rho^\mu) \bar{\mathcal{H}}] + i\lambda \text{Tr} [\mathcal{H} \sigma_{\mu\nu} F^{\mu\nu} \bar{\mathcal{H}}]\end{aligned}$$

- $Z_c$  as a virtual state ranged from -35 to -15 MeV (which mainly the  $\sigma$  coupling  $g_s$ )
- The pion coupling  $g_a$  fixed by  $D^* \rightarrow D\pi$
- Then we obtain a pole position distribution of  $G(3900)$



# Robustness of our conclusion- correction contribution

## Coupled-channel calculation

TABLE SM-III. The comparison between the poles of  $G(3900)$  within the single-channel case and the coupled-channel calculation involving  $D\bar{D}$ ,  $D\bar{D}^*/\bar{D}D^*$  and  $D^*\bar{D}^*$  (in units of MeV).

$\Lambda$ (GeV)	0.5	0.6	0.7
Single channel	$-4.0 - 27.3i$	$2.0 - 27.3i$	$7.0 - 24.4i$
Coupled channel	$-0.1 - 25.0i$	$6.3 - 21.4i$	$9.7 - 12.6i$

## The DDpi three-body effect

$$q_0 = E - p_0 - p'_0$$

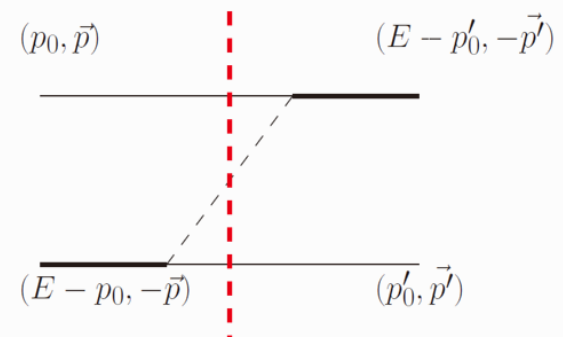


TABLE SM-IV. The impact of the three-body  $D\bar{D}\pi$  effect from the OPE of  $D\bar{D}^* \rightarrow \bar{D}D^*$  on the pole of  $G(3900)$  (in units of MeV).

$\Lambda$ (GeV)	0.5	0.6	0.7
Without 3-body effect	$-4.0 - 27.3i$	$2.0 - 27.3i$	$7.0 - 24.4i$
With 3-body effect	$-5.0 - 24.1i$	$-1.2 - 24.3i$	$6.3 - 21.7i$

# Robustness of our conclusion- correction contribution

## Recoil correction

$$V_{\sigma}^{D(recoil)}(\mathbf{p}', \mathbf{p}) = -\frac{1}{2m_{D^*}^2} \frac{g_s^2}{\mathbf{q}^2 + m_{\sigma}^2} ((\boldsymbol{\epsilon} \cdot \mathbf{q})(\boldsymbol{\epsilon}' \cdot \mathbf{q}) - i\mathbf{S} \cdot \mathbf{L}),$$

$$\begin{aligned} V_{\pi/\eta}^{C(recoil)}(\mathbf{p}', \mathbf{p}) &= -\frac{g^2}{2f_{\pi}^2} \frac{1}{\mathbf{k}^2 - k_0^2 + m_{\pi/\eta}^2} \\ &\times \left[ -\frac{m_{D^*}^2 - m_D^2}{2m_{D^*}^2} i\mathbf{S} \cdot \mathbf{L} \right. \\ &- \frac{(m_{D^*} - m_D)^2 (\boldsymbol{\epsilon} \cdot \mathbf{q})(\boldsymbol{\epsilon}' \cdot \mathbf{q})}{4m_{D^*}^2} - (\boldsymbol{\epsilon} \cdot \mathbf{k})(\boldsymbol{\epsilon}' \cdot \mathbf{k}) \end{aligned}$$

$$\times \frac{3m_{D^*}^2 - 2m_{D^*}m_D - m_D^2}{4m_{D^*}^2} \left. \times \begin{cases} \tau \cdot \tau, & \text{for } \pi, \\ \mathbb{1} \cdot \mathbb{1}, & \text{for } \eta, \end{cases} \right]$$

$$\begin{aligned} V_{\rho/\omega}^{D(recoil)}(\mathbf{p}', \mathbf{p}) &= \frac{1}{\mathbf{q}^2 + m_{\rho/\omega}^2} \\ &\times \left[ \left( \frac{-\lambda\beta g_V^2}{2m_{D^*}} + \frac{\beta^2 g_V^2}{8m_{D^*}^2} \right) (\boldsymbol{\epsilon} \cdot \mathbf{q})(\boldsymbol{\epsilon}' \cdot \mathbf{q}) \right. \\ &+ \left( \frac{\lambda\beta g_V^2(m_{D^*} + m_D)}{2m_D m_{D^*}} - \frac{\beta^2 g_V^2}{8m_{D^*}^2} \right) i\mathbf{S} \cdot \mathbf{L} \\ &\left. + \frac{\beta^2 g_V^2}{16m_{D^*}m_D} \mathbf{k}^2 (\boldsymbol{\epsilon}' \cdot \boldsymbol{\epsilon}) \right] \times \begin{cases} \tau \cdot \tau, & \text{for } \rho, \\ \mathbb{1} \cdot \mathbb{1}, & \text{for } \omega, \end{cases} \end{aligned}$$

$$\begin{aligned} V_{\rho/\omega}^{C(recoil)}(\mathbf{p}', \mathbf{p}) &= \frac{1}{\mathbf{k}^2 - k_0^2 + m_{\rho/\omega}^2} \\ &\times \left[ \frac{\lambda^2 g_V^2 (m_{D^*} - m_D)^2}{4m_{D^*}m_D} \mathbf{q}^2 (\boldsymbol{\epsilon}' \cdot \boldsymbol{\epsilon}) \right. \\ &+ \frac{\lambda^2 g_V^2 (2m_{D^*} + m_D)(m_{D^*} - m_D)^2}{4m_{D^*}^3} (\mathbf{q} \cdot \boldsymbol{\epsilon})(\mathbf{q} \cdot \boldsymbol{\epsilon}') \\ &+ \frac{\lambda^2 g_V^2 m_D (m_{D^*}^2 - m_D^2)}{2m_{D^*}^3} i\mathbf{S} \cdot \mathbf{L} \\ &+ \frac{\lambda^2 g_V^2 (m_{D^*} - m_D)^2}{4m_{D^*}m_D} \times (\mathbf{k} \cdot \boldsymbol{\epsilon})(\mathbf{k} \cdot \boldsymbol{\epsilon}') \\ &+ \frac{\lambda^2 g_V^2 (m_{D^*} - m_D)^2 (2m_{D^*} + m_D)}{4m_{D^*}^3} \\ &\left. \times \mathbf{k}^2 (\boldsymbol{\epsilon}' \cdot \boldsymbol{\epsilon}') \right] \times \begin{cases} \tau \cdot \tau, & \text{for } \rho, \\ \mathbb{1} \cdot \mathbb{1}, & \text{for } \omega, \end{cases} \end{aligned}$$

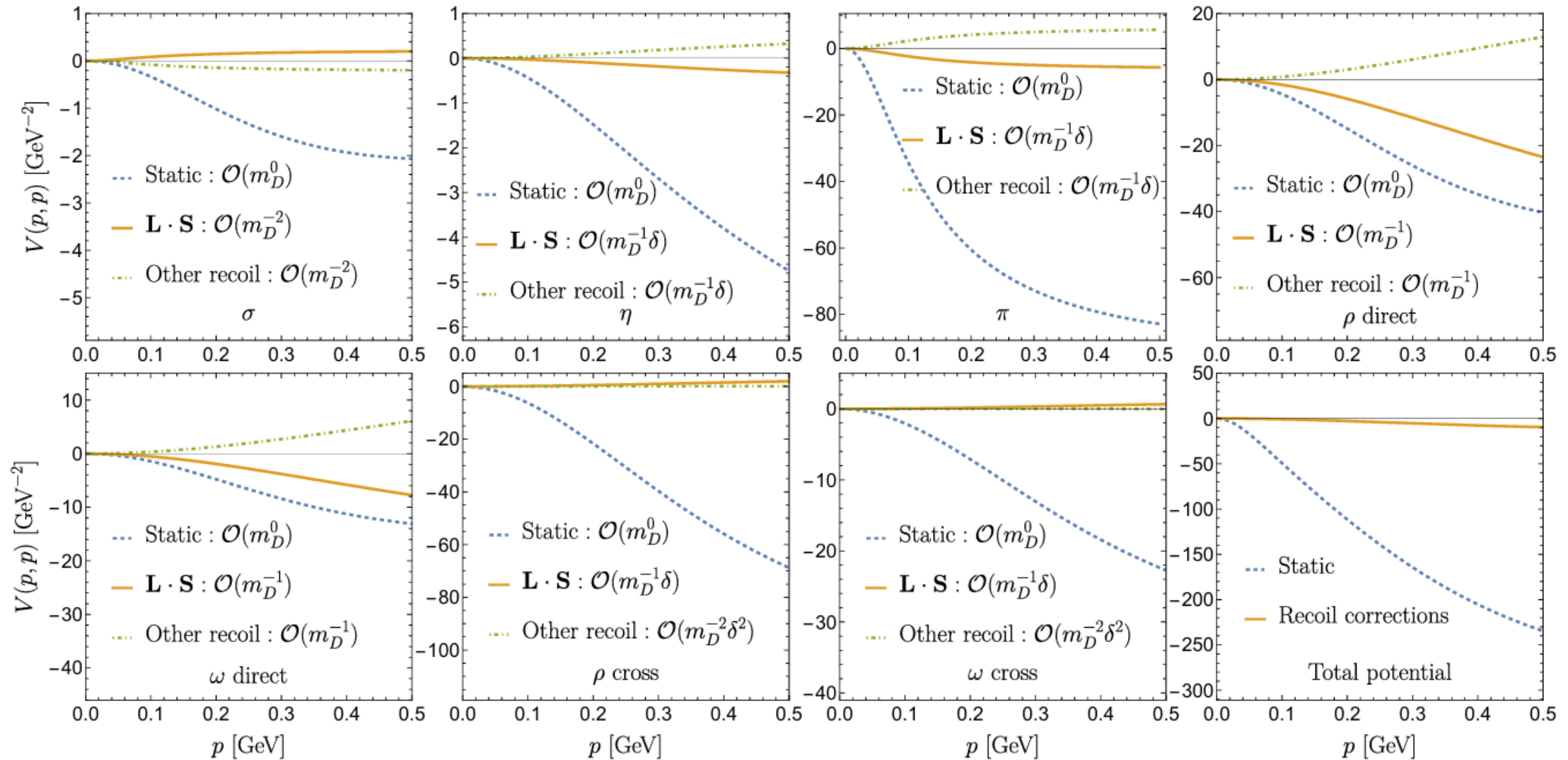
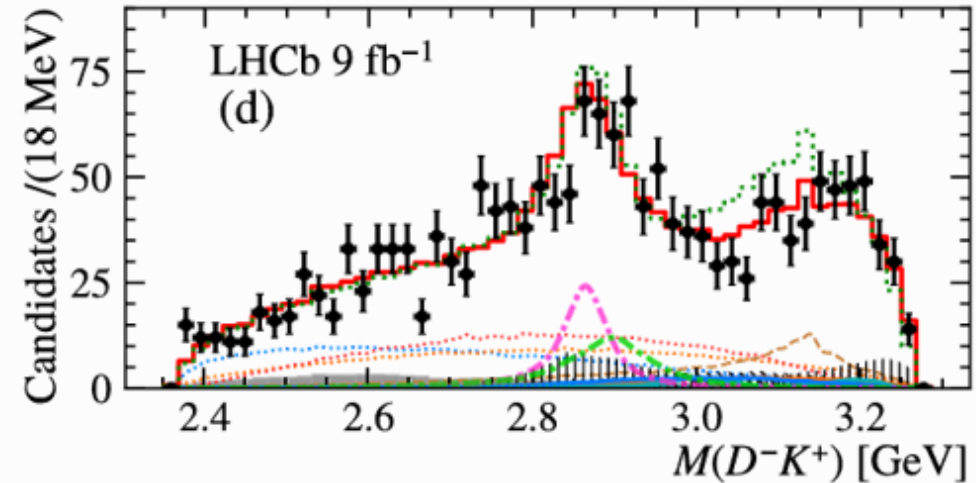
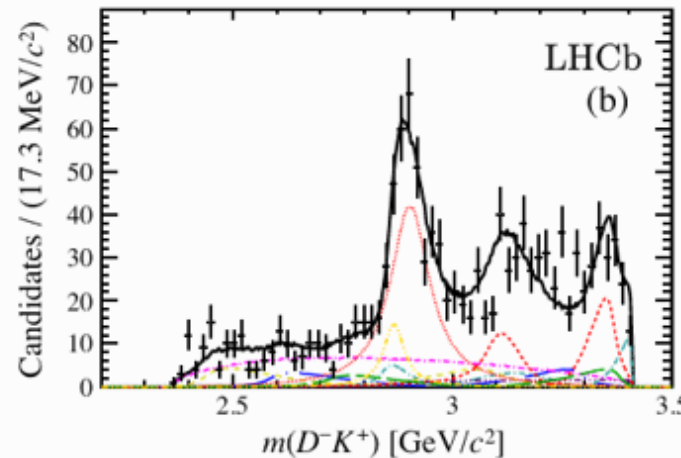


FIG. S7. The explicit recoil corrections for the  $P$ -wave effective potential of the  $D\bar{D}^*$  associated with  $G(3900)$  up to the order of  $1/m_D^2$ . Here, the  $\delta = m_{D^*} - m_D$  is another small scale. Only  $p = p'$  cases are depicted.

# Extension: $X_1(2900)$ as the P-wave $\bar{D}^* K^*$ resonance



$$J^P = 0^+ \quad \textcolor{blue}{T_{\bar{c}\bar{s}0}^*(2900)^0} \quad \textcolor{blue}{T_{\bar{c}\bar{s}1}^*(2900)^0} \quad J^P = 1^-$$

$$m_0 \quad 2866 \pm 7 \quad 2904 \pm 5$$

$$\Gamma_0 \quad 57 \pm 13 \quad 110 \pm 12$$

$$T_{\bar{c}\bar{s}0}^*(2900)^0 \quad T_{\bar{c}\bar{s}1}^*(2900)^0$$

$$2887 \pm 10 \quad 2914 \pm 19$$

$$92 \pm 23 \quad 128 \pm 32$$

(LHCb Collaboration), Phys. Rev. D 102, 112003 (2020)

(LHCb Collaboration), Phys. Rev. Lett. 133, 131902 (2024)

- $X_0(2900)$  &  $X_1(2900)$  seem a pair of S-wave and P-wave molecules like  $X(3872)$  &  $G(3900)$

# Double pole structure: $X_1(2900)$ as the P-wave $\bar{D}^*K^*$ resonance

- $X_0(2900), X_1(2900)$  and an additional  $1^-$  state

$$T_{cs0}(2900) \sim {}^1S_0$$

$$T_{cs1}(2900) \sim {}^1P_1 + {}^5P_1$$

$$T'_{cs1}(2900) \sim {}^3P_1$$

- Dependency on the unknown parameter  $\lambda'$

States	$\lambda' = 0.56$	$\lambda' = 0.28$	$\lambda' = 0.84$
$T_{cs0+}(2900)$	2.859*	2.878*	2.833*
	$2.857 - 0.012i$	$2.876 - 0.016i$	$2.832 - 0.008i$
$T_{cs1-}(2900)$	$2.834 - 0.037i^*$	$2.835 - 0.052i^*$	$2.840 - 0.028i^*$
	$2.828 - 0.054i$	$2.827 - 0.069i$	$2.834 - 0.045i$
$T'_{cs1-}(2900)$	$2.868 - 0.028i^*$	$2.869 - 0.033i^*$	$2.869 - 0.024i^*$
	$2.861 - 0.049i$	$2.862 - 0.054i$	$2.862 - 0.045i$

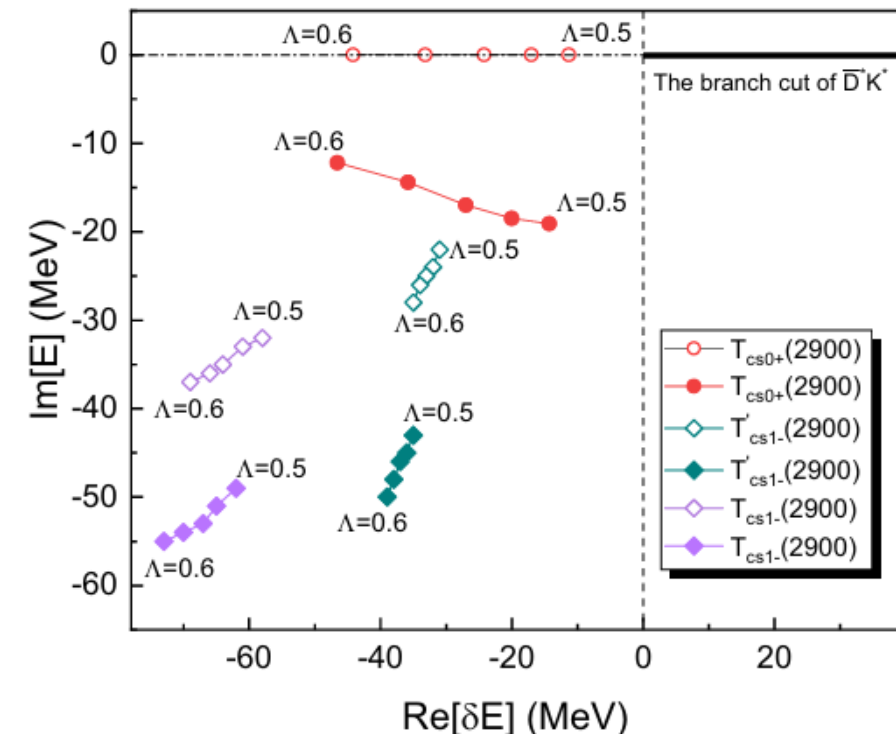


FIG. 2. The pole trajectories of S-wave  $T_{cs0+}(2900)$ , P-wave  $T_{cs1-}(2900)$  and  $T'_{cs1-}(2900)$  with the varying cutoff parameter  $\Lambda$  from 0.5 to 0.6 GeV. Here, the circle and diamond points correspond to the poles in the physical and unphysical Riemann sheets, respectively. The hollow and solid points represent the results without and with the width effect of the  $K^*$  meson, respectively.

# Summary and outlook

- Model-based calculation: unified description of  $X(3872)$ ,  $T_{cc}^+$ ,  $Z_c(3900)$  and  $G(3900)$ , with additional states predicted
- Robustness from the pion exchange and P-wave mechanism and small influence from various effects
- P-wave scattering dynamics exhibit new behaviors compared to S-wave hadron-hadron scattering.
- STCF will be an excellent platform to study the general behaviors of P-wave hadron-hadron scattering dynamics, which involves various systems such as charmed and anti-charmed meson, charmed and anti-charmed baryon, and double charmonium scattering.

**Thanks for your attention!**